# Microstructural Characterization of a Pt-Aluminide Coated IN738LC

*I. Calliari, M. Dabalà, and A. Zambon*

*(Submitted 7 December 1999; in revised form 4 January 2000)*

**In this paper, the microstructural and chemical characterization of the IN738LC superalloy, coated with a Pt-Cr modified aluminide coating, is presented. The effects of aging in air at 850 °C on superalloy and coating microstructures were investigated. The growth of $\gamma'$ precipitates in IN738LC follows the Wagner-Lifshits model. The positive effect of Pt in preventing refractory element diffusion into the outer coating is not influenced by the aging. A moderate precipitation of TCP phases has been noted at the coating-superalloy interface.**

**Keywords** aging, aluminide coating, microstructure, nickel alloy IN738LC, platinum-modified coatings

## 1. Introduction

Given the extremely aggressive conditions in the combustion environment of industrial gas turbines, some fuel and atmospheric contaminants, such as sulfur and chlorine, cause accelerated oxidation and hot corrosion attack of Ni-base superalloys turbine components, operating at temperatures as high as 900 °C. To increase the useful service life for the components, hot corrosion resistant coatings have been studied and produced. Aluminide coatings,[1,2] obtained *via* the pack cementation process, are commonly employed to protect $\gamma'$-strengthened Ni-based blades. The pack normally consists of the coating element source, an activator, usually a halide salt, and an inert filler material, often alumina, to prevent the source of sintering at high temperature. Solid-state diffusion, when the element source reacts with the substrate alloy, and gas phase diffusion of the halides of this element are the main phenomena involved in coating formation. Typically, the outer coating layer is formed of $\beta$-NiAl and a solid solution of elements originating from the substrate. By adding platinum, the protective nature of aluminide coating is significantly improved. In this case, the outer coating contains intermetallic phases such as $PtAl_2$, $Pt_2Al_3$, or PtAl.[3,4] Platinum increases the coating stability toward inward diffusion of aluminum or outward diffusion of nickel, and prevents refractory transition elements such as Mo, V, and W from diffusing into the outer coating layers[5,6] and eliminates the Cr-rich precipitates in the outer coating layers.[7]

**I. Calliari, M. Dabalà,** and **A. Zambon,** Department of Mechanical and Management Innovation (DIMEG), University of Padua, 35131 Padova, Italy. Contact e-mail: irene.calliari@unipd.it.

In this study, the microstructural and chemical characterization of the IN738LC superalloy, coated with a commercially produced (RT22 type) Pt-Cr[8] modified aluminide coating (Pt deposited by electroplating and codeposition of Cr-Al by the pack cementation process), is presented. The effects of aging on superalloy and coating microstructures were investigated after heat treatment at 850 °C for 500 to 2000 h.

## 2. Materials and Methods

The composition of IN738LC superalloy is reported in Table 1. The samples were aged at 850 °C in air for 500, 1000, 1500, and 2000 h. All the specimens were characterized using a scanning electron microscope (SEM, Cambridge Stereoscan 440) equipped with an energy dispersive spectrometer (EDS, PV9800) and a CDU® detector, (Philips Electronic Instruments Corp., Mahwah, NJ). For the phase quantitative analysis, an electron beam current of 500 pA, a voltage of 25 kV, and a standardless procedure with ZAF (Z (atomic number) Absorption Fluorescence) correction were employed. The accuracy of the method was checked on the bulk of the same superalloy. For the line profiles across the coating, the IMIX® system (Princeton Gamma Tech., NJ) was employed. The microstructure was investigated after chemical (Kalling's etchant) and electrolytic etchings ($H_3PO_4$ 20 vol.% aqueous solution for 10 s at 3 V). The EDS analysis and line profiles were performed without etching.

## 3. Results and Discussion

### 3.1 IN738LC

The microstructure of a new and an aged (2000 h) sample of IN738 are reported in Fig. 1 and 2, and the $\gamma'$ (cuboidal

**Table 1 Chemical composition (wt.%) of IN738LC**

| Cr | Co | Ti | Al | W | Ta | Mo | Nb | Zr | B | C | Ni |
|---|---|---|---|---|---|---|---|---|---|---|---|
| 15.7–16.3 | 8.0–9.0 | 3.2–3.7 | 3.2–3.7 | 2.4–2.8 | 1.5–2.0 | 1.5–2.0 | 0.6–0.11 | 0.06–0.10 | 0.008–0.014 | 0.09–0.13 | Bal |

and spherical) and $\gamma''$ spherical precipitates are evident. The sizes of $\gamma'$ and $\gamma''$ have been evaluated on SEM micrographs by means of a computerized image analysis procedure. In Table 2, the mean diameter values ($d$) of $\gamma'$ and $\gamma''$ and the corresponding standard deviation ($\sigma$) are reported.

Coarsening of fine precipitates is generally explained with the volume diffusion-controlled theory formulated by Lifshits and Wagner. This model[9] proposes that the mean particle diameter ($d$) increases with aging time ($t$) according to the equation

$$(d^3 - d_0^3)^{1/3} = \mathrm{k} \times t^{1/3}$$

where $k$ is related to the diffusion coefficient of $\gamma'$ solutes in $\gamma$, to the $\gamma/\gamma'$ interfacial free energy, to the equilibrium molar concentration of $\gamma'$ in $\gamma$, and to the aging temperature. The reported data follow this model quite well, as indicated in Fig. 3, with a value of $k = 1.7$ nm/s$^{1/3}$, confirming the trends reported in other studies.[9,10,11] The coarsening of $\gamma'$ induces a decrease of the hardness values, from 425 HV (new sample) to 350 HV (1000 h). As the volume fraction of $\gamma'$ and $\gamma''$ remains constant, the mean particle distance increases with aging, so that the hindrance to dislocations' movements is progressively decreased.

The SEM micrograph in Fig. 4 shows the interface between the coating and the alloy substrate of the sample treated for 500 h, with the TCP phases. The EDS spectrum taken on these phases shows an increase in Cr compared to the surrounding "bulk" phases. The PHACOMP calculation, performed on the "as-received" sample (Nv [mean value] = 2.38), confirms that the IN738LC is not prone to TCP precipitation. The term Nv is the alloy mean number of unpaired electrons.

On the contrary, EDS determination performed on the as-received sample, in the 10 $\mu$m wide zone close to the coating and consequent PHACOMP computation, showed that the Nv is 2.7, which is consistent with the observed TCP phases in the treated samples. The presence of these phases is related to the high Cr concentration in the interdiffusion zone, due to the Al-Cr pack cementation process.[6,8,12]

The SEM investigations confirmed that most of the carbides are located at grain boundaries, at which only a few intragranular carbides were detected. The former improve the creep resistance, as they control the grain boundary slipping. Comparing the SEM images of as-received and aged samples, it can be

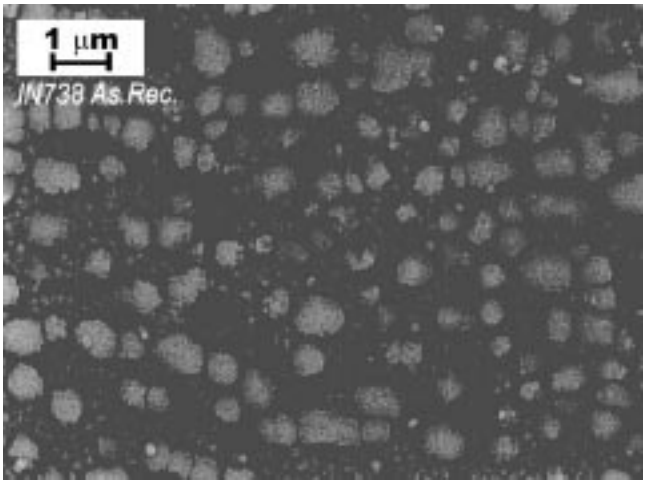


**Fig. 1** $\gamma'$ phase of IN 738LC sample as-received

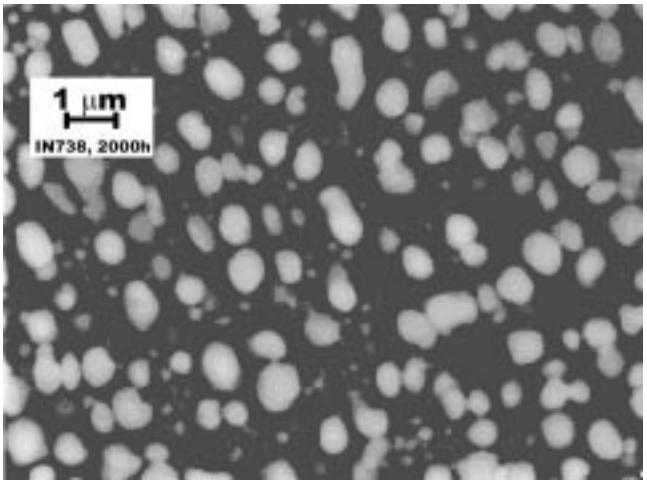


**Fig. 2** $\gamma'$ phase of IN 738LC sample aged for 2000 h

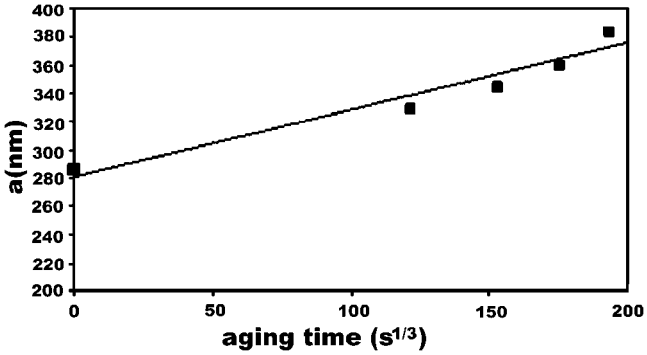


**Fig. 3** Plot of primary $\gamma'$ phase growth vs aging time, according to the Wagner model ($a$ = radius of precipitate)

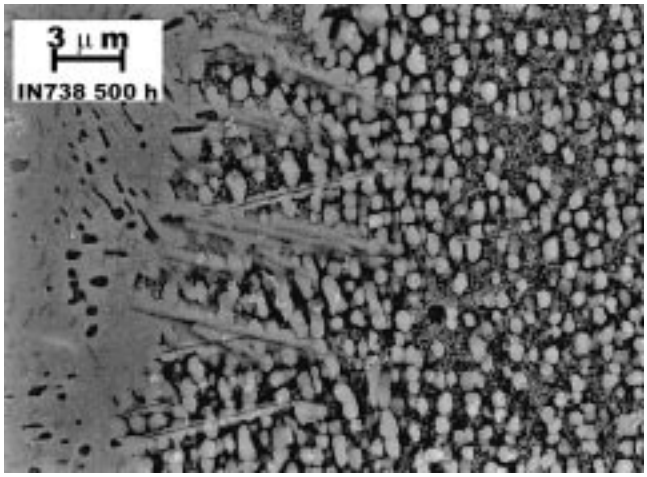


**Fig. 4** TCP platelike sigma phase precipitation at the coating-superalloy interface in the sample aged for 500 h

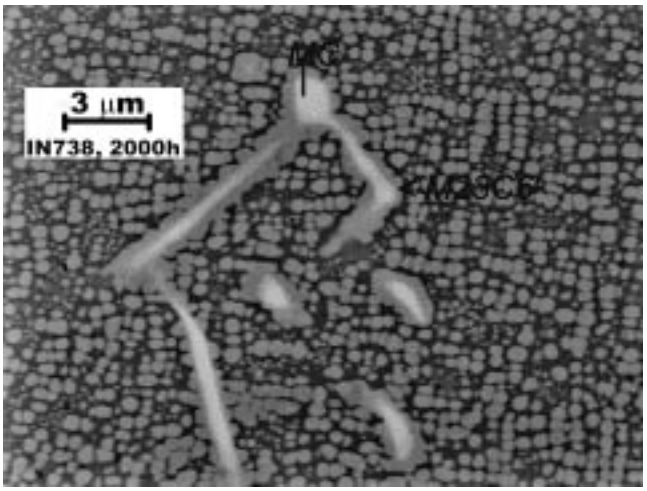


**Fig. 5** Evolution of MC carbides both into $\gamma'$ phase and $M_{23}C_6$ carbides in a sample aged for 2000 h

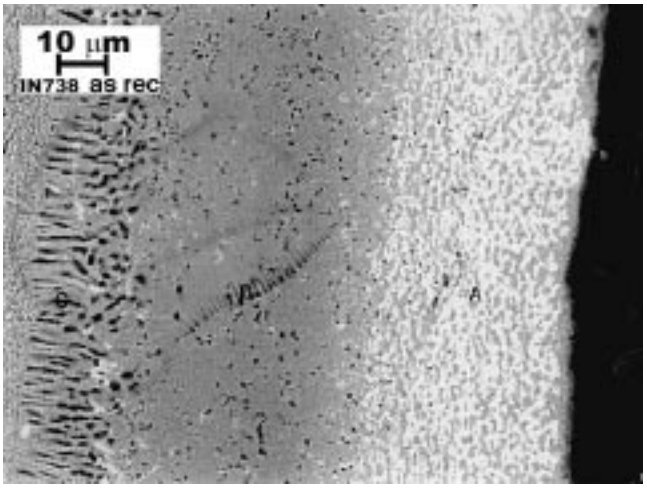


**Fig. 6** SEM image of coating in the as-received condition. A: Pt-rich zone, B: Pt partially substitutes for Al to form $\beta$-Ni(PtAl) phase, and C: some Cr-rich precipitates. The crack is in the embedding resin

**Table 2 Mean values of the diameters of $\gamma'$ and $\gamma''$ (nm) and corresponding standard deviations**

| | As-received | 500 h | 1000 h | 1500 h | 2000 h |
|---|---|---|---|---|---|
| $d$ ($\gamma'$) | 570 | 660 | 690 | 720 | 770 |
| $\sigma$ | 12 | 11 | 11 | 9 | 8 |
| $d$ ($\gamma''$) | 160 | 180 | 210 | 230 | 270 |
| $\sigma$ | 3 | 3 | 4 | 4 | 10 |

deduced that the aging induces a small increase of the intergranular carbides and an evolution of MC carbides. During the heat treatment, these precipitates react with the $\gamma$-matrix according to

$$MC + \gamma \rightarrow M_{23}C_6 + \gamma'$$

In Fig. 5, the MC (light area) carbide is surrounded by $\gamma'$

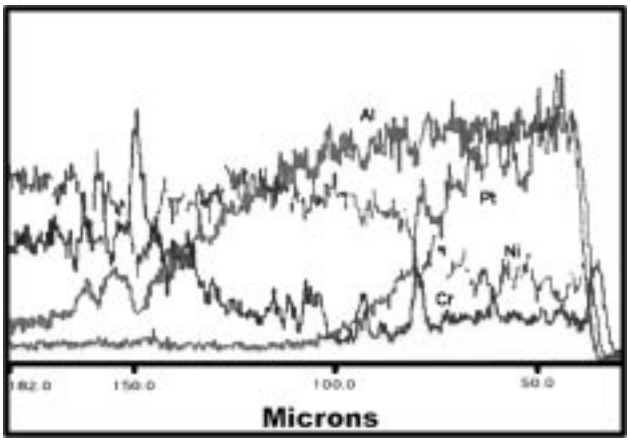


**Fig. 7** Line profiles taken on the coating of the as-received sample

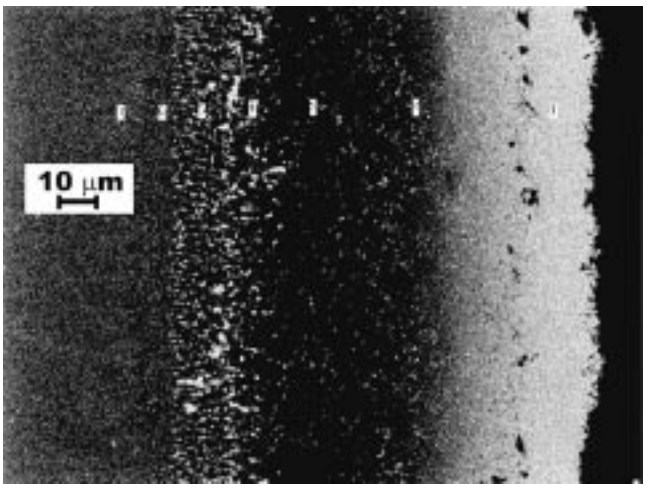


**Fig. 8** Coating of the superalloy sample aged for 2000 h. The superimposed numbers show the positions where quantitative EDS analysis was performed

and small $M_{23}C_6$ carbides.[13] The EDS data confirm that MC contains Ti and Ta, while the sorrounding $M_{23}C_6$ contains Cr and Mo.

### 3.2 Coating

In order to verify the reliability of the determinations of the local compositions by EDS on heat-treated samples, preliminary standardless quantitative analysis obtained with ZAF correction was performed on a bulk sample of IN738LC in the as-received condition (Table 3).

Deviations of less than 5 to 10% were noted for all the elements whose atomic number was higher than 13 (aluminum). Therefore, the accuracy of the method is suitable for the analysis of very complex phases, if the stoichiometric coefficients need not be determined exactly.

In Fig. 6, the scanning electron microscope-backscattered electron micrograph of the as-received sample is shown (the crack on the right side belongs to the embedding resin); the coating thickness is about 120 $\mu$m, as confirmed by the Al-line profile (Fig. 7). The Pt-rich outer zone A (20 to 25 $\mu$m)

**Table 3 Quantitative EDS analysis of IN738LC (wt.%)**

| | Cr | Co | Ti | Al | W | Ta | Mo | Nb | Zr | B | C | Ni |
|---|---|---|---|---|---|---|---|---|---|---|---|---|
| EDS-ZAF | 15.7 | 8.6 | 3.6 | 4.1 | 2.4 | 2.0 | 1.9 | 0.8 | n.d. | n.d. | n.d. | Bal |
| Composition range | 15.7–16.3 | 8.0–9.0 | 3.2–3.7 | 3.2–3.7 | 2.4–2.8 | 1.5–2.0 | 1.5–2.0 | 0.6–1.1 | 0.06–0.10 | 0.008–0.014 | 0.09–0.13 | Bal |

**Table 4 Compositions (at.%) and probable phases in the areas indicated in Fig. 8 (s.s. = solid solution)**

| | Al | Pt | Ti | Cr | Co | Ni | Mo | W | Phases |
|---|---|---|---|---|---|---|---|---|---|
| P1 as-received | 57.2 | 20.3 | 0.3 | 1.6 | 3.3 | 13.6 | … | … | PtAl, $PtAl_2$, $Pt_2Al_3$, NiAl |
| P1 2000 h | 48.6 | 9.0 | 0.3 | 1.4 | 4.0 | 36.7 | … | … | NiAl, PtAl, $PtAl_2$ |
| P2 as-received | 52.5 | 3.8 | 0.7 | 4.5 | 3.7 | 34.8 | … | … | NiAl, $PtAl_2$, $(Cr, Co)_{s.s.}$ |
| P2 2000 h | 47.1 | 0.4 | 1.0 | 4.2 | 5.3 | 42.0 | … | … | NiAl, $(Cr, Co)_{s.s.}$ |
| P3 as-received | 43.3 | … | 1.5 | 7.2 | 4.8 | 43.0 | … | 0.3 | NiAl, $(Cr, Co)_{s.s.}$ |
| P3 2000 h | 43.3 | … | 2.5 | 5.7 | 6.6 | 41.8 | … | … | NiAl, $(Cr, Co)_{s.s.}$ |
| P4 as-received | 31.1 | … | 4.1 | 7.8 | 5.9 | 50.9 | 0.3 | 0.2 | NiAl, carbides |
| P4 2000 h | 32.4 | … | 4.1 | 16.7 | 7.2 | 38.1 | 0.4 | 1.0 | NiAl, carbides |
| P5 as-received | 15.7 | … | 4.5 | 25.0 | 7.6 | 42.5 | 2.4 | 2.3 | NiAl, carbides |
| P5 2000 h | 18.9 | … | 5.8 | 24.8 | 8.5 | 35.1 | 3.0 | 3.0 | NiAl, $\alpha$-Cr, carbides |
| P6 as-received | 11.9 | … | 4.8 | 19.6 | 8.9 | 53.2 | 1.0 | 0.7 | NiAl, $\gamma$ and $\gamma'$, $\alpha$-Cr |
| P6 2000 h | 13.5 | … | 4.7 | 20.2 | 7.9 | 50.5 | 1.5 | 1.2 | $\gamma$ and $\gamma'$, TCP phases |
| P7 as-received | 8.7 | … | 4.0 | 19.9 | 7.7 | 57.2 | 1.4 | 1.1 | $\gamma$ and $\gamma'$ |
| P7 2000 h | 10.4 | … | 4.3 | 18.6 | 8.7 | 54.7 | 1.5 | 1.2 | $\gamma$ and $\gamma'$ |

**Table 5 $HV_{0.2}$ values obtained on the coating**

| Distance from surface ($\mu$m) | HV (mean) | SD | HV (mean) | SD | HV (mean) | SD | HV (mean) | SD | HV (mean) | SD |
|---|---|---|---|---|---|---|---|---|---|---|
| | As-received | | 500 h | | 1000 h | | 1500 h | | 2000 h | |
| 10 | 747 | 170 | 608 | 19 | 485 | 13 | 470 | 9 | 470 | 21 |
| 60 | 521 | 11 | 437 | 16 | 549 | 43 | 512 | 7 | 457 | 17 |
| 110 | 833 | 44 | 732 | 18 | 664 | 11 | 639 | 34 | 620 | 12 |
| 120 | 626 | 10 | 688 | 35 | 670 | 29 | 716 | 28 | 562 | 33 |
| 150 | 430 | 17 | 432 | 15 | 361 | 23 | 384 | 20 | 363 | 19 |

contains fine precipitates (small bright particles) of $PtAl_2$, $Pt_2Al_3$, and PtAl in a matrix of $\beta$-NiAl; in the B zone (60 to 65 $\mu$m), the amount of intermetallic phases decreases and Pt partially substitutes for Al to form $\beta$-Ni(PtAl) phase. Some Cr-rich precipitates, which can be identified[4] as $\alpha$-Cr, were detected in the C zone (25 to 30 $\mu$m). The A and B layers are free of refractory elements (Mo and W). From the data reported in Table 4 (points 1 to 4 belong to A and B zones) and from the micrographs in Fig. 8, W, Mo, and $\alpha$-Cr precipitates are absent in the outer layers, both in new and aged samples, which is a significant effect of the protective role of the Pt-modified coating.

The aging and concomitant hot oxidation have no effect on the thickness of the coating, but determine an evolution of the phase compositions, as can be deduced from line profiles (Fig. 7) and from data reported in Table 4. The numbers superimposed in Fig. 8 indicate the positions where quantitative analyses (investigated area 2 × 2 $\mu$m) were performed, both in as-received and 2000 h aged samples. By considering the composition determinations and structure morphology, an identification of probable phases is proposed, whose results are reported in Table 4.

In Table 5, the hardness values of new and aged samples are reported. The measurements were performed in five points, at a depth of 10 $\mu$m (outer layer of the coating), 60 $\mu$m (center of the coating), 110 $\mu$m (columnar zone), 120 $\mu$m (interface between the columnar zone and the substrate), and 150 $\mu$m (substrate).

The microhardness values distribution, certainly affected by diffusion, coalescence of precipitates, and precipitation of new ones, shows a decrease of the peak values with increasing heating time, so that the final hardness values generally appear to be lower than the original ones. Such a decrease in hardness and lack in the TCP phases of elements involved in the mechanism of solid solution strengthening, probably reduce the embrittlement effect of these phases present at the coating-superalloys interface, in samples aged for 2000 h.

The hardness values near the surface decrease after 500 h of aging, probably due to the increasing of volume fraction of the ductile $\beta$-(Ni, Pt)Al phase content as Al diffuses outward to form $Al_2O_3$ and Ni diffuses from the bulk to the coating.

## 4. Conclusions

In this study, it was verified that the positive effects of Pt on the stability of aluminide coating are not influenced by air aging at 850 °C for 2000 h. The aging has no effect on the

thickness of the coating, but determines an evolution of the phase composition with a moderate outward diffusion of Ni and a moderate inward diffusion of Al.

The extension of the precipitation of TCP phases at the interface is limited, which reduces the harmful effects on the material strength, while the hardness decreases with soaking time. The growth of $\gamma'$ precipitates follows the Wagner criteria.

## References


1. R. Streiff: in *Elevated Temperature Coatings: Science and Technology II*, N.B. Dahotre, and J.M. Hampikian, eds., TMS, Warrendale, PA, 1996, pp. 407-16.
2. R. Mevrel, C. Duret, and R. Pichoir: *Mater. Sci. Technol.*, 1986, vol. 2, pp. 201-6.
3. M.F. Stroosnijeder, M.J. Bennett, and R. Mevrel: in *Advanced Techniques for Surface Engineering*, W. Gissler, and H.A. Jehn, eds., Kluwer Academic Publishers, Dordrecht, The Netherlands, 1992, pp. 335-58.
4. H.M. Tawancy, N.M. Abbas, and T.N. Rhys-Jones: *Surf. Coating Technol.*, 1991, vol. 49, pp. 1-7.
5. T.N. Rhys-Jones, and N. Swindells: *Mater. Sci. Eng.*, 1987, pp. 389-97.
6. M.R. Jackson, and J.R. Rairden: *Metall. Trans. A*, 1977, vol. 8A, pp. 1697-707.
7. J.H. Sun, H.C. Jang, and E. Chang: *Surf. Coating Technol.*, 1994, vol. 64, pp. 195-203.
8. G.H. Marijnissen: in *High Temperature Protective Coatings*, S.C. Singhal, ed., TMS-AIME, Warrendale, PA, 1983, pp. 27-35.
9. R.A. Stevens, and P.E. Flewitt: *Mater. Sci. Eng.*, 1979, vol. 37, pp. 237-47.
10. D. McLean: *Met. Sci.*, 1984, vol. 18, pp. 249-56.
11. Y. Yoshioka, N. Okabe, T. Okamura, D. Saito, K. Fujiyama, and H. Kashiwaya: *Superalloys*, R.D. Kissinger, *et. al.*, eds., TMS, 1996, pp. 173-79.
12. W.F. Gale, and J.E. King: *Mater. Sci. Technol.*, 1986, vol. 2, pp. 201-06.
13. G.P. Sabol, and R. Stickler: *Phys. Status Solidi*, 1969, vol. 35 (11), pp. 11-52.